

Optical study of segregation effects on the electronic properties of molecular-beam-epitaxy grown (In,Ga)As/GaAs quantum wells

P. Disseix, J. Leymarie, A. Vasson, A.-M. Vasson, and C. Monier

Laboratoire des Sciences et Matériaux pour l'Electronique, et d'Automatique, Unité de Recherche Associée au Centre National de la Recherche Scientifique No. 1793, Université Blaise-Pascal Clermont-Ferrand II, 63177 Aubière Cedex, France

N. Grandjean, M. Leroux, and J. Massies

Centre de Recherche sur l'Hétéro-Epitaxie et ses Applications, Centre National de la Recherche Scientifique, Rue Bernard Grégory, Sophia-Antipolis, 06560 Valbonne, France

(Received 19 July 1996)

Indium segregation in $\text{In}_x\text{Ga}_{1-x}\text{As}/\text{GaAs}$ ($0.3 < x \leq 0.5$) quantum wells grown by molecular-beam epitaxy and its influence on their electronic properties are investigated using thermally detected optical absorption. A kinetic model is used to derive concentration profiles and applied to interpret experimental data. The dependence of the In surface segregation on growth temperature and growth rate is studied. It is shown that a decrease of the substrate temperature is the best method to limit the segregation process kinetically. From a fit of the kinetic model to experimental data, the conduction-band offset ratio Q_c is found to be independent of indium composition x between 0.2 and 0.5 ($Q_c = 0.64 \pm 0.01$). The exciton wave function is calculated using a variational technique involving a transfer-matrix formalism to study the influence of potential shape on excitonic properties. Only a slight increase in oscillator strength with In segregation is observed for the fundamental excitonic transition. [S0163-1829(97)06104-3]

I. INTRODUCTION

Strained layer structures offer two main advantages over lattice-matched systems for device realization. First, different band-gap ranges are achievable through the greater freedom in choice of alloy composition, and, second, the strain splitting of the valence band at the Γ point enables valence-band engineering to take place. In the case of (In,Ga)As/GaAs, it is well known that the biaxial compression of the $\text{In}_x\text{Ga}_{1-x}\text{As}$ material lifts the degeneracy at the top of valence band. The uppermost valence-band component is derived from the bulk heavy-hole band and presents a relatively small effective mass for motion in the plane of the layer.¹ This has been exploited in devices made from $\text{In}_x\text{Ga}_{1-x}\text{As}/\text{GaAs}$ strained quantum well structures in high-speed electronics or optoelectronics.²⁻⁴

However, there are several limits inherent to the $\text{In}_x\text{Ga}_{1-x}\text{As}/\text{GaAs}$ system. For an indium concentration greater than 0.2, the (In,Ga)As growth is, in a first stage, bi-dimensional (2D) and then becomes tri-dimensional (3D). The 2D-3D transition in the growth mode involves the formation of islands which are elastically relaxed.⁵⁻⁸ Then plastic relaxation through dislocation generation occurs as the (In,Ga)As thickness is increased. Moreover, it is now well established that, during the growth of an $\text{In}_x\text{Ga}_{1-x}\text{As}/\text{GaAs}$ heterostructure by molecular-beam epitaxy (MBE), surface segregation of In constitutes an ultimate limitation to the achievement of perfectly abrupt interfaces.⁹⁻¹⁵ Optical measurements display a strong ability to probe the interfacial quality of $\text{In}_x\text{Ga}_{1-x}\text{As}/\text{GaAs}$ quantum wells (QW's) since electronic states are sensitive to the profile of the In composition.^{12,16} However, a correct interpretation of the spectroscopic data needs a theory for segregation to model the In distribution at the GaAs/ $\text{In}_x\text{Ga}_{1-x}\text{As}$ and

$\text{In}_x\text{Ga}_{1-x}\text{As}/\text{GaAs}$ interfaces. For this purpose, different approaches have been proposed^{10,12,17,18} but only the method of Grandjean, Massies, and Leroux,¹⁷ based on a Monte Carlo simulation of the growth, and the kinetic model of Dehaese, Wallart, and Mollot¹⁸ are able to provide the variation of the In composition profile as a function of growth parameters; the others fail in predicting correct profile variations with substrate temperatures and growth rates.

In this paper, we report a quantitative analysis of the effects of In segregation on the optical and electronic properties of $\text{In}_x\text{Ga}_{1-x}\text{As}/\text{GaAs}$ QW's as functions of growth conditions. We use the kinetic approach of Dehaese, Wallart, and Mollot¹⁸ for the analysis of thermally detected optical-absorption (TDOA) results on $\text{In}_x\text{Ga}_{1-x}\text{As}/\text{GaAs}$ QW's grown by MBE under various conditions of temperature and growth rate. To our knowledge, it is the first time that this particular model has been used to account for experimental data. It leads to an explicit description of the variation of electronic states as a function of the growth parameters. The fit of the calculated transition energies of heavy-hole and light-hole excitons (e_1hh_1 and e_1lh_1 , respectively) to the measured values enables the strained conduction-band offset ratio (Q_c) to be determined. Q_c is chosen as an adjustable parameter together with the In composition and other parameters entering the model. Experimental measurements by various groups¹⁹⁻²⁴ have yielded different results for Q_c which is a key parameter for tailoring the optical and electronic properties of devices. From the examination of several samples, we determine Q_c for different values of the indium concentration (x). The result is in agreement with a simple calculation based on potential deformation theory and on the properties of the (In,Ga)As alloy. The last part of this paper is concerned with the effect of the indium segregation in (In,Ga)As/GaAs heterostructures on the excitonic properties

TABLE I. Nominal growth parameters of the samples investigated.

Sample	x	T_g (°C)	V_g (ML s ⁻¹)	L_w (ML)
1	0.35	400	0.50	6-8-10-12-16
2	0.35	450	0.50	6-8-10-12-16
3	0.35	500	0.50	6-8-10-12-16
4	0.35	500	1.30	6-8-10-12-16
5	0.5	530	0.60	4
6	1.0	450	0.18	1.1 (×4)

and particularly on the oscillator strength of the transitions.

II. EXPERIMENTAL DETAILS

A. Growth conditions and calibration

In_xGa_{1-x}As/GaAs QW samples have been grown on n^+ -type doped (001) GaAs substrates in an MBE machine equipped with an *in situ* reflection high-energy electron-diffraction (RHEED) facility. After the growth of a GaAs buffer layer at 580 °C, the substrate temperature was reduced to a value between 400 and 530 °C to obtain the In_xGa_{1-x}As QW's. Further details on the growth can be found in Ref. 7; the nominal indium composition (x), growth temperature (T_g), growth rate (V_g), and QW thickness (L_w) are listed in Table I. The samples, labeled 1, 2, 3, and 4, contain five quantum wells with different thicknesses separated by 400-Å-thick barriers and samples 5 and 6 are single quantum wells. Growth rates, QW thicknesses and indium compositions were determined accurately by the variation in the RHEED specular beam intensity. For the segregation study, we focus our analysis on the experimental results obtained on samples 1–4 which have the same In composition but correspond to different growth parameters.

B. Thermally detected optical-absorption experiments

TDOA at liquid-helium temperatures is very appropriate to detect small absorption signals arising from ultrathin layers. Its use in the characterization and for the study of semi-conducting QW structures has been demonstrated previously (e.g., Refs. 25 and 24 at liquid ⁴He and ³He, respectively).

In this technique, the heating of the sample caused by the phonon emission due to nonradiative deexcitation, which occurs after optical absorption, is detected via a thermometer maintained with the sample at low temperature. The monochromatic excitation source consists of a halogen lamp followed by a HR640 Jobin-Yvon monochromator. The thermometer is a germanium resistor shielded from the incident radiation. A bolometer enables the TDOA spectra to be normalized. The resistance variations of the thermometer and of the bolometer are detected by using ac Wheatstone bridges and lock-in amplifiers. The TDOA sensitivity increases drastically when the temperature is lowered because of the decrease of the specific-heat capacity of the sample-holder-thermometer assembly and of the increase in the thermometer sensitivity. The results reported here are from experiments carried out at about 0.35 K by using an adsorption ³He refrigerator which was implanted into the ⁴He bath

cryostat employed in previous TDOA studies. Further details about the experimental setup can be found in Refs. 25 and 26.

III. THEORETICAL MODELING

A. Kinetic model for the indium segregation

In order to determine the indium composition profile in (In,Ga)As/GaAs QW's, we use the kinetic approach developed by Deahese, Wallart, and Molloy.¹⁸ In this model, the segregation is described by an exchange process between a Ga surface atom and an In atom in the bulk phase. This exchange process must overcome the energy barrier E_1 with a rate $P_1 = \nu_0 \exp(-E_1/kT_g)$, where $\nu_0 = 10^{13} \text{ s}^{-1}$ is the vibration frequency. The reverse exchange can also occur: the rate P_2 is given by $\nu_0 \exp(-E_2/kT_g)$, but the corresponding energy barrier E_2 is larger. The difference $E_2 - E_1 = E_s$ corresponds to the segregation energy of the equilibrium model.¹⁰ The time evolution of the number of In surface atoms is obtained from the balance of incoming and outgoing In atoms. Thus,

$$dX_{\text{In } s}/dt = \Phi_{\text{In}} + P_1 X_{\text{In } b}(t) X_{\text{Ga } s}(t) - P_2 X_{\text{In } s}(t) X_{\text{Ga } b}(t), \quad (1)$$

where Φ_{In} is the In flux in monolayers per second (ML s⁻¹). The numbers of In and Ga atoms, $X_{\text{In } i}(t)$ and $X_{\text{Ga } i}(t)$, at the surface ($i=s$) or in the bulk ($i=b$), are expressed in fractions of monolayers. The second term of the right-hand side of Eq. (1) represents those In atoms which leave the bulk phase (b) for the surface layer (s). It is expressed as the rate P_1 weighted by the number of exchange possibilities which are taken to be product $X_{\text{In } b}(t) X_{\text{Ga } s}(t)$. In the same way, the reverse exchange results in a number of In atoms leaving the surface phase given by $P_2 X_{\text{In } s}(t) X_{\text{Ga } b}(t)$. Furthermore, the conservation of In and total surface atoms during the time interval $[0, t]$ gives

$$X_{\text{In } s}(0) + X_{\text{In } b}(0) + \Phi_{\text{In}} t = X_{\text{In } s}(t) + X_{\text{In } b}(t), \quad (2)$$

$$X_{\text{In } s}(0) + X_{\text{Ga } s}(0) + (\Phi_{\text{In}} + \Phi_{\text{Ga}}) t = X_{\text{In } s}(t) + X_{\text{Ga } s}(t). \quad (3)$$

Since $X_{\text{In } b}(t) + X_{\text{Ga } b}(t) = 1$, the combination of the three equations above leads to a differential equation for $X_{\text{In } s}(t)$. A numerical solution of this equation with a predictor-corrector method enables the In concentration profile to be deduced.²⁷

B. Electronic states and excitonic properties

The calculation of confinement energies in the QW heterostructures is carried out within the framework of the effective-mass approximation. The energies of the electron, heavy- or light-hole levels in a QW modified by In segregation are determined within the transfer-matrix formalism including the strain effects on the (In,Ga)As band structure. The physical constants of GaAs and InAs used in the calculations are specified in Table I of Ref. 24 and are the result from a careful analysis of data available in the literature. The physical constants of In_xGa_{1-x}As are calculated by a linear interpolation between binary values, except for electron and light-hole effective masses for which the strain-induced

modification along the quantization axis of the QW is considered.²⁸ For the strain-free band gap of $\text{In}_x\text{Ga}_{1-x}\text{As}$, we use the expression given by Goetz *et al.*:²⁹ E_g (eV) = $1.5192 - 1.5837x + 0.475x^2$ at 2 K.

In order to evaluate the effect of a gradual potential due to In segregation on the excitonic properties developed in Sec. IV D, the transfer-matrix formalism was combined with a variational method.^{30,31} However, to ensure computational rapidity, several assumptions have been made. Valence-band mixing effects^{32,33} were not included in the calculation and a trial excitonic envelope function with a single variational parameter, a_b , has been chosen. It is expressed as follows:

$$\phi = \varphi_e(z_e)\varphi_h(z_h)\exp[-\sqrt{r^2 + (z_e - z_h)^2}/a_b]. \quad (4)$$

z_e and z_h are, respectively, the coordinates of the electron and hole along the quantization axis and r is the relative distance between the two particles in the layer plane. $\varphi_e(z_e)$ and $\varphi_h(z_h)$ are the envelope functions related to the electrons and holes in the quantum well. Indeed, it has been shown that, for the thicknesses corresponding to the QW's investigated, the introduction of a second variational parameter does not modify greatly the results of the calculation in comparison with these obtained by using only one parameter.³⁰

IV. RESULTS AND DISCUSSION

A. TDOA spectra

The TDOA spectra of samples 1 and 2 are displayed in Figs. 1(a) and 1(b) in the range of the QW emission wavelengths. The continuous increase of the TDOA signal with the increase of the photon energy is due to the impurity absorption front of the GaAs barriers in both cases. The excitonic absorption in GaAs is detected at 1.515 eV in each sample. In order to obtain precise values of the energies of the different excitonic absorption peaks, the baseline, mainly due to the GaAs absorption front and also including band-to-band contributions of the QW transitions, has been removed by simulating it with a polynomial curve. The results of the subtraction of this baseline from the TDOA signal, displayed in each figure after amplification, enable the energy of each peak to be determined accurately. The fundamental excitonic transition e_1hh_1 is detected for all the QW thicknesses of 6, 8, 10, 12, 16 ML's. The electron-light-hole transition is only observed for the 6- and 8-ML-wide QW's. One can easily measure the energy shifts of the different absorption peaks of sample 2 with respect to those of sample 1 which have been grown with the same rate but at a lower temperature (see Table I). The effect of segregation is to increase the transition energies¹² and appears to be much less important for sample 1. This can be explained in terms of kinetic limitation of segregation at low growth temperatures.¹⁸ It will be shown in the following section that this behavior can be quantified by using the kinetic model presented above. Finally, one can note a smaller energy shift between the absorption peaks attributed to the e_1lh_1 transition observed in samples 1 and 2. Light holes are less sensitive to segregation effects due to a large extension of their envelope wave function with respect to the scale of the In gradual repartition. Furthermore, their levels are quasis resonant to the GaAs valence band.

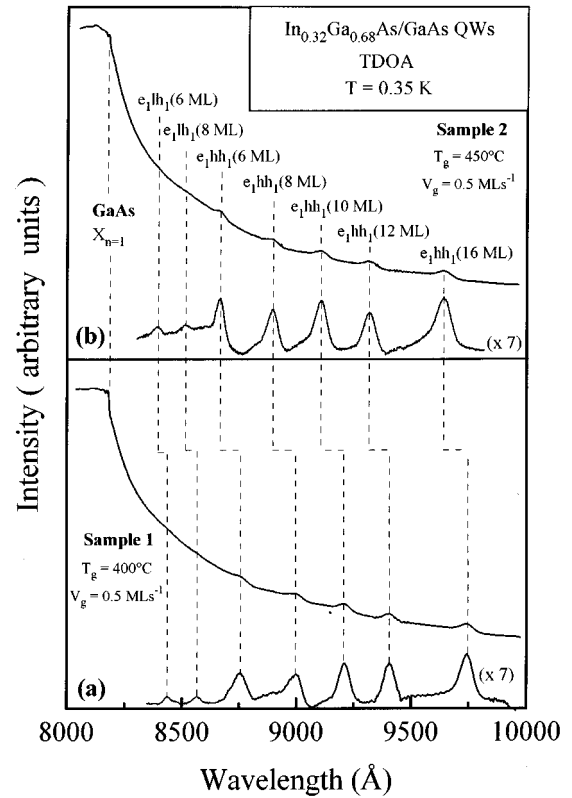


FIG. 1. TDOA spectra of $\text{In}_x\text{Ga}_{1-x}\text{As}/\text{GaAs}$ multiple quantum wells ($x \approx 0.32$) obtained at 0.35 K. The upper part of the figure concerns sample 2 grown at 450°C with a rate of 0.5 ML s^{-1} and the lower part corresponds to sample 1 grown with the same growth rate but at a lower temperature ($T_g = 400^\circ\text{C}$). The e_1hh_1 and e_1lh_1 excitonic absorption signals have been amplified for each sample after the removal of the GaAs absorption front (see text for details). The dashed lines are guides for the eyes. Note the redshift of the excitonic transitions (sample 1) with the decrease of the substrate temperature. The excitonic transition in the GaAs barriers is also detected.

B. Analysis of the data

The procedure which consists of eliminating the GaAs absorption from the TDOA spectra, has been systematically used in order to obtain the absorption energies values. The accurate determination of the e_1hh_1 and e_1lh_1 energies provides an experimental data set enabling the validity of the kinetic model to be demonstrated. The experimental energies are displayed as functions of QW thickness for samples 1–4 in Fig. 2. On the lower part of this figure (part a), we have plotted together the results from samples 1 and 2, which have been grown with the same rate but at different temperatures. The upper part [Fig. 2(b)] concerns the results of samples 3 and 4 obtained at the same growth temperature but with different growth rates.

In order to obtain the fit of the calculations within the kinetic model to the experimental data, the adjustable parameters considered were E_1 , $E_2 = E_1 + E_s$, the conduction band offset ratio Q_c , and the indium concentration x . A slight variation of this last parameter was allowed around the nominal value estimated from RHEED measurements. The well thicknesses are assumed to be accurately controlled. The growth parameters (T_g and V_g) used for the calculations are

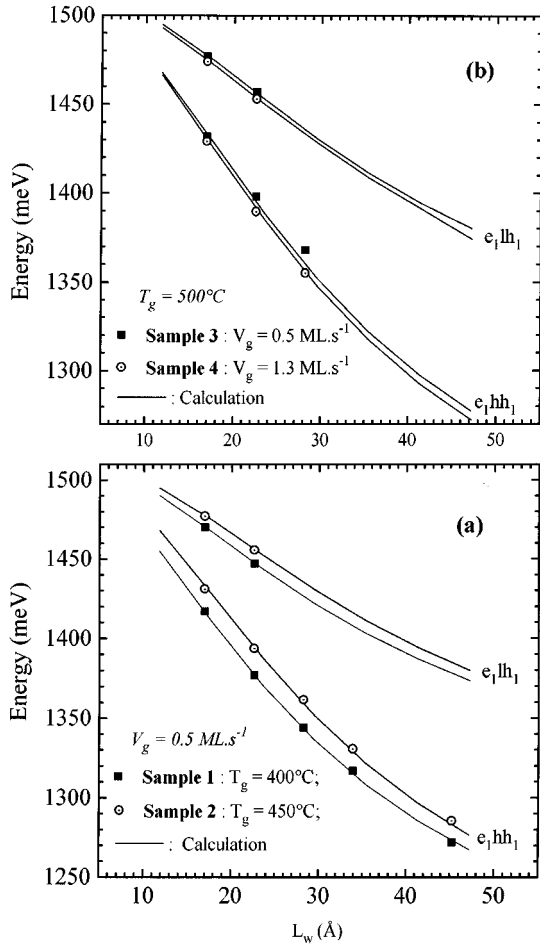


FIG. 2. Thickness dependence of the excitonic transition energies for samples 1,2 (a) and 3,4 (b). ■ and ○ represent the experimental energies and the solid lines are the results of calculations based on the kinetic model and including the nominal growth parameters (T_g and V_g) indicated in the figure for each sample. The theoretical results are displayed for the fit parameters: $E_1=1.73$ eV, $E_s=0.13$ eV, $Q_c=0.64$ eV, and $x=0.32\pm 0.01$.

those measured during the growth (see Table I). The choice of Q_c as an adjustable parameter is justified by the observation of the e_1lh_1 transition which is rather sensitive to this value for the thinnest QW's. The ground-state level of the light holes, which resides near the top of the well, is indeed strongly dependent on the exact depth of the valence-band well.

Inspection of Fig. 2 shows that

(i) There is a good agreement between the theoretical curves (solid lines) and the experimental points for all the samples, proving the ability of the kinetic model to account for the variation of the In composition profile versus growth parameters. The shifts in the transition energies, when the growth temperature is increased [Fig. 2(a)] or when the growth rate is decreased [Fig. 2(b)], are well predicted. The parameters leading to the best fit to all experimental data are $E_1=(1.73\pm 0.02)$ eV, $E_s=(0.13\pm 0.01)$ eV, $Q_c=0.64\pm 0.01$, and $x=0.32\pm 0.01$. For a given parameter, except E_1 , the uncertainty is the maximum deviation between the value given above and these obtained from the individual fits for each sample. For E_1 , only the samples grown at the lowest temperatures were used; for the samples fabricated at

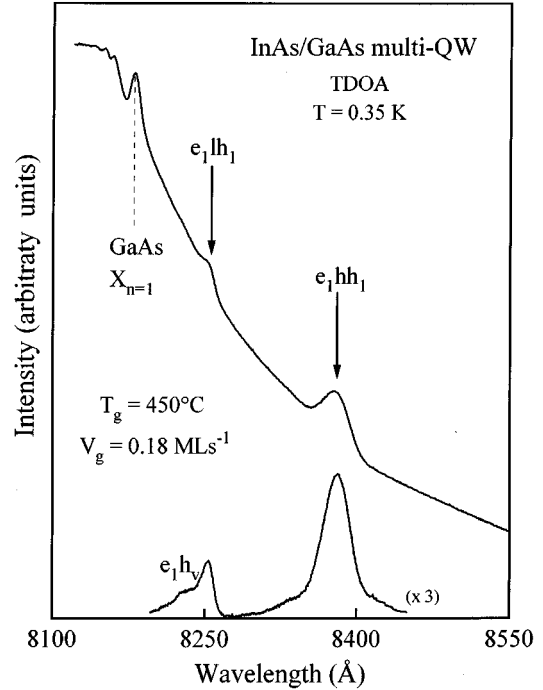


FIG. 3. TDOA spectrum of an InAs/GaAs multiple quantum well sample grown at 450°C with a low growth rate (0.18 ML s^{-1}). As in Fig. 1, the e_1hh_1 and the e_1lh_1 excitonic absorptions have been amplified after removing the GaAs front absorption (vertical amplification ratio given in the lowest part of the figure). The vertical arrows show the theoretical transition energies between electron and heavy- or light-hole ground states after the correction for the exciton binding energy, calculated with $E_1=1.73$ eV, $E_s=0.13$ eV, and $Q_c=0.64$ for a QW thickness adjusted to 1.07 ML.

500°C , E_1 can change significantly without altering the fit. The value for E_s determined here is in reasonable agreement with previous surface analysis studies on (In,Ga)As alloys which have yielded an estimate of E_s ($E_s=0.15\pm 0.1$ eV).¹⁰

(ii) The use of the same set of values for the adjustable parameters E_1 and E_2 for all samples demonstrates the reliability of the In segregation model for $\text{In}_x\text{Ga}_{1-x}\text{As}/\text{GaAs}$ heterostructures.

(iii) A decrease in the growth temperature of 50°C at a given growth rate of 0.5 ML s^{-1} [Fig. 2(a)] has more of an effect than an increase of the growth rate from 0.5 to 1.3 ML s^{-1} at $T_g=500^\circ\text{C}$ [Fig. 2(b)]. When the substrate temperature decreases without any variation in the growth rate, the flux term is no longer negligible with respect to the exchange terms in Eq. (1) and consequently, there is a kinetic limitation of segregation. The model is also able to predict variations of the In segregation with growth rates, but such an effect is weak at 500°C [Fig. 2(b)] because, with a growth rate of approximately 1 ML s^{-1} , the exchange terms are always greater than the flux term. The system is then near thermodynamical equilibrium so that In concentration profiles are weakly sensitive to variations in the growth rate.

We have also tested the model on a multiple-quantum well structure which contains four InAs/GaAs QW's each of 1 ML thickness, grown at 450°C and 0.18 ML s^{-1} (sample 6). Figure 3 displays TDOA spectra obtained from this sample. The signals corresponding to the e_1hh_1 and e_1lh_1 excitonic transitions are clearly detected. A weak band on the

high-energy side of the e_1lh_1 excitonic peak is also observed. It is labeled e_1h_v because it involves transitions between confined electrons in the InAs well and unconfined holes in the GaAs barrier continuum. Since light holes are weakly localized in the InAs layer and quasiresonant with the GaAs valence-band edge, the small energy difference (~ 4.5 meV) between the e_1h_v and e_1lh_1 peaks must be related to the binding energy of light-hole excitons. In Fig. 3, we have shown the theoretical e_1hh_1 and e_1lh_1 excitonic energies (vertical arrows) calculated with $E_1=1.73$ eV, $E_s=0.13$ eV, and $Q_c=0.64$ i.e., same as above) for a QW thickness adjusted to 1.07 ML (closed to the nominal thickness=1.1 ML). Good agreement between the calculated and experimental energies is obtained by strictly using the growth rate and temperature parameters measured during the growth. However, at 450 °C and at a growth rate of 0.18 ML s⁻¹, the exchange terms are relatively important with respect to the flux term and there is no efficient kinetic limitation of segregation. At this temperature, a sensible reduction of the segregation process would need a growth rate above 1 ML s⁻¹. It must be noted that the maximum indium composition in the well is only 0.3 due to segregation so that the corresponding data is in the range of the indium compositions investigated here.

C. Strained conduction-band offset ratio

The band offset of the (In,Ga)As/GaAs system has been investigated extensively during the past few years through the analysis of the electronic states of strained In_xGa_{1-x}As/GaAs quantum wells by optical spectroscopy experiments. For this purpose, the strained conduction-band offset ratio Q_c was introduced as an adjustable parameter in the models used to calculate the QW energy levels. An important advantage in using this parameter lies in the fact that neither the pressure coefficient of the valence band nor the distribution of the alloy band gap bowing between conduction and valence bands have to be known.

The fit to our experimental data enables us to determine Q_c with accuracy. For the samples investigated here with $x=0.32$ and $x=0.5$ (sample 5), we find that Q_c is constant and is equal to 0.64 ± 0.01 . The same value was deduced previously from an analysis of TDOA and reflectivity measurements carried out on In_{0.22}Ga_{0.78}As/GaAs QW's of various thicknesses.²⁴ We then deduce that Q_c is independent of the indium composition for x between 0.2 and 0.5. This behavior can be justified by a simple model within potential deformation theory, based on the knowledge of the unstrained InAs/GaAs valence-band offset (V_0) and the distribution of the (In,Ga)As band gap bowing between valence and conduction bands. By taking $a_v = -(a_c - a_v)/10$, which is a reasonable value^{34,35} (a_c is the hydrostatic deformation potential of the conduction band and a_v that corresponding to the valence band), an excellent agreement is found with the experimental data for $V_0=0.140$ eV by assuming that 25% of the alloy band gap bowing is assigned to the valence band (see Fig. 4). These last results are found to be in agreement with a previous experimental determination of V_0 (Ref. 36) and theoretical calculations concerning the (In,Ga)As alloy.³⁷

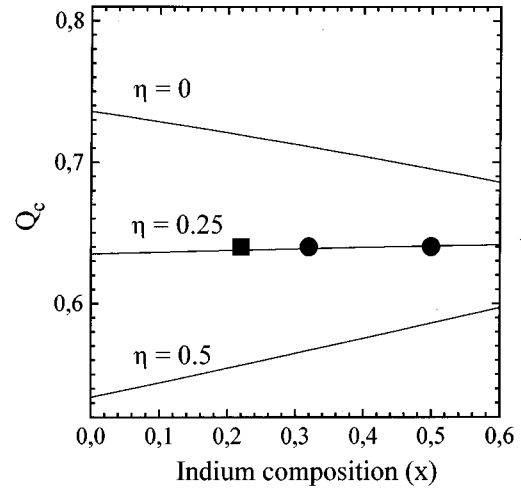


FIG. 4. The conduction-band offset ratio Q_c as a function of the indium composition. The experimental data (●: this work, ■: Ref. 24) are compared with theoretical calculations (straight lines) using an unstrained valence-band offset $V_0=0.140$ eV and different values (η) of the bowing band-gap part assigned to the valence band. Good agreement is found with the experimental data for $\eta=0.25$.

D. Segregation effects on excitonic properties

The influence of In surface segregation on excitonic energies in In_xGa_{1-x}As/GaAs QW's has already been in evidence from optical studies since these energies are sensitive to the potential profile at the interfaces. However, the effect of the segregation on the excitonic oscillator strengths (f_{osc}), has, to our knowledge, never been studied previously. The oscillator strength of the e_1hh_1 excitonic transition in an ideal (In,Ga)As/GaAs QW is compared with that corresponding to the same quantum well whose potential profile is modified by the indium segregation. The calculation of the excitonic envelope wave function is performed with the variational principle by using the transfer-matrix formalism.

The oscillator strength per unit area is

$$f_{osc} \propto \left| \int_{-\infty}^{\infty} \phi(z_e=z, z_h=z, r=0) dz \right|^2 / \langle \phi | \phi \rangle$$

$$= \left| \int_{-\infty}^{\infty} \varphi_e(z) \varphi_h(z) dz \right|^2 / \langle \phi | \phi \rangle, \quad (5)$$

here $\phi(z_e, z_h, r)$ is the exciton wave function given in Sec. III B. The behavior of f_{osc} is thus determined by the variations of the overlap of electron and hole wave functions and of the normalization term $\langle \phi | \phi \rangle$ which depends on the in-plane exciton Bohr radius a_b .

The relative variations of f_{osc} , with respect to the oscillator strength in a square QW, are given in Table II for different In concentrations and QW thicknesses. The indium segregation chosen here corresponds to the usual MBE growth conditions i.e., $V_g=0.5$ ML s⁻¹ and $T_g=500$ °C. The parameters of the kinetic model are those previously determined ($E_1=1.73$ eV, $E_s=0.13$ eV). Note that the calculations are carried out for QW thicknesses which are below the critical thickness or the thickness corresponding to the 2D-3D growth mode transition for x larger than 0.2.

TABLE II. Variations (in %) of the oscillator strength of the e_1hh_1 excitonic transition due to segregation in usual MBE growth conditions for QW's of different sizes and In concentrations.

L_w (ML) \ x	0.1	0.2	0.3	0.5
2	9.0	9.0	9.0	10.5
4	7.5	6.0	6.0	8.5
8	3.0	1.0	1.5	2.0
12	0.0	-0.5		
16	-1.0	-0.5		
24	-0.5			

It appears that segregation does not modify significantly the oscillator strength of the e_1hh_1 excitonic transition. This result is interpreted by considering the envelope wave functions of the electron and the hole, i.e., $\varphi_e(z_e)$ and $\varphi_h(z_h)$. For the quantum well thicknesses investigated, the extension of the wave function is much larger than a typical extent of the indium distribution (~ 30 Å) and the variation of the integral $\int \varphi_e(z)\varphi_h(z)dz$ is not large. As an example, the products $\varphi_e(z)\varphi_h(z)$ without and with segregation are compared to the gradual profile of the indium incorporation in a 2 ML QW with a nominal composition x of 0.5 as shown in Fig. 5. The oscillator strength in a QW with segregation is generally greater than that in a perfect square QW. Since segregation has no significant effect on the exciton Bohr radius and, consequently, on the normalisation term $\langle \phi | \phi \rangle$, the variation of f_{osc} is mainly due to the more important overlap of the electron and hole envelope functions in a QW with segregation.

V. CONCLUSION

TDOA measurements have been carried out in order to study optical properties of $\text{In}_x\text{Ga}_{1-x}\text{As}/\text{GaAs}$ QW's grown by MBE under various growth conditions. The TDOA data have been interpreted by using envelope function calculations based on a kinetic model for building In composition profiles, which includes explicitly the growth parameters (rate or temperature). In accordance with the experimental results, this model accounts well for the variation of In segregation with substrate temperature or growth rate. This work suggests that kinetics can be used to limit the In segregation process during the $\text{In}_x\text{Ga}_{1-x}\text{As}/\text{GaAs}$ QW growth. It demonstrates that a way to limit segregation is to prevent the system from reaching thermodynamic equilibrium by us-

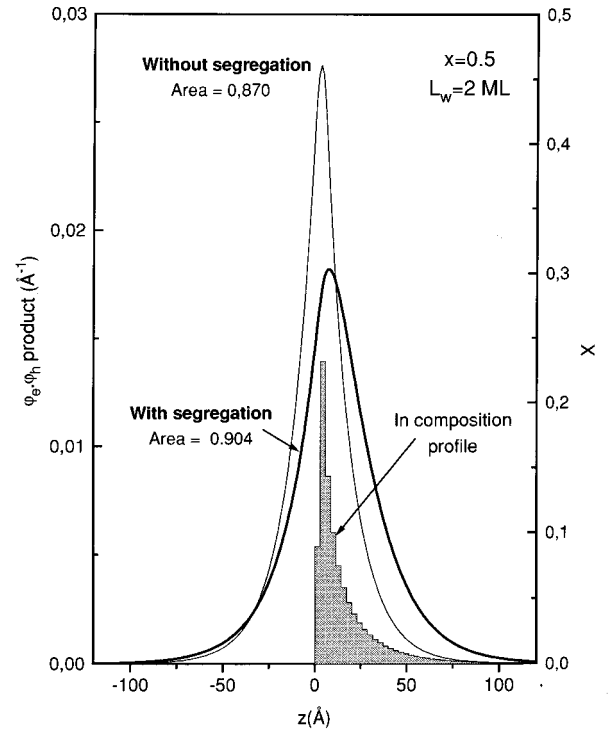


FIG. 5. The product of the normalized electron and hole envelope functions versus the distance z in a two ML $\text{In}_{0.5}\text{Ga}_{0.5}\text{As}/\text{GaAs}$ QW without and with In surface segregation together with the In composition profile calculated for standard MBE growth conditions: $T_g=500$ °C, $V_g=0.5$ ML s^{-1} for $E_s=0.13$ eV and $E_1=1.73$ eV. The areas below each curve, which correspond to the envelope function overlap ($\int \varphi_e(z)\varphi_h(z)dz$), are also indicated.

ing low growth temperatures or high growth rates. However, the substrate temperature seems to be the most efficient parameter to limit kinetically the exchange process. In addition, the fit to our experimental data set enables the conduction-band offset ratio ($Q_c=0.64\pm 0.01$) to be determined accurately and in agreement with previous results obtained for $x=0.2$. We have then deduced its independence of the In composition in the range of x from 0.2 to 0.5. This result is in agreement with a simple calculation based on the potential deformation theory and assuming that 25% percent of the alloy band-gap bowing is assigned to the valence band. The effect of segregation on exciton quantization, particularly on the oscillator strength of the e_1hh_1 excitonic transition, has also been studied by using a variational technique within the transfer-matrix formalism. Our numerical results indicate a slight increase of the oscillator strength with segregation which is explained in terms of envelope function overlap.

¹G. C. Osbourn, J. Vac. Sci. Technol. B **4**, 1423 (1986).

²J. M. Ballingall, P. Ho, G. J. Tessler, P. A. Martin, N. Lewis, and E. L. Hall, Appl. Phys. Lett. **54**, 2121 (1989).

³N. Chand, E. E. Becker, J. P. Van der Ziel, S. N. G. Chu, and N. K. Dutta, Appl. Phys. Lett. **58**, 1704 (1991).

⁴T. R. Chen, B. Zhao, Y. H. Zhuang, A. Yariv, J. E. Ungar, and S. Oh, Appl. Phys. Lett. **60**, 1782 (1992).

⁵S. Guha, A. Madhukar, and K. C. Rajkumar, Appl. Phys. Lett. **57**, 2110 (1990).

⁶C. W. Snyder, B. G. Orr, D. Kessler, and L. M. Sander, Phys. Rev. Lett. **66**, 3032 (1991).

⁷N. Grandjean and J. Massies, J. Cryst. Growth **134**, 51 (1993).

⁸N. Grandjean, J. Massies, M. Leroux, J. Leymarie, A. Vasson, and A. M. Vasson, Appl. Phys. Lett. **64**, 2664 (1994).

- ⁹J. Massies, F. Turco, A. Salètes, and J. P. Contour, *J. Cryst. Growth* **80**, 307 (1987).
- ¹⁰J. M. Moison, C. Guille, F. Houzay, F. Barthe, and M. Van Rompay, *Phys. Rev. B* **40**, 6149 (1989).
- ¹¹J. M. Gerard and J. Y. Marzin, *Phys. Rev. B* **45**, 6313 (1992).
- ¹²K. Muraki, S. Fukatsu, Y. Shiraki, and R. Ito, *Appl. Phys. Lett.* **61**, 557 (1992).
- ¹³J. Nagle, J. P. Landesman, M. Larive, C. Mottet, and P. Bois, *J. Cryst. Growth* **127**, 550 (1993).
- ¹⁴J. M. Gerard, C. d'Anterrosches, and J. Y. Marzin, *J. Cryst. Growth* **127**, 536 (1993).
- ¹⁵H. Yu, C. Roberts, and R. Murray, *Appl. Phys. Lett.* **66**, 2253 (1995).
- ¹⁶C. Monier, J. Leymarie, A. Marti Ceschin, N. Grandjean, A. Vasson, A. M. Vasson, M. Leroux and J. Massies, *J. Phys (France) IV* **3**, C5-295 (1993).
- ¹⁷N. Grandjean, J. Massies, and M. Leroux, *Phys. Rev. B* **53**, 998 (1996).
- ¹⁸O. Dehaese, X. Wallart, and F. Mollot, *Appl. Phys. Lett.* **66**, 52 (1995).
- ¹⁹Q. Xu, Z. Y. Xu, J. Z. Xu, B. Z. Zheng, and H. Xia, *Solid State Commun.* **73**, 813 (1990).
- ²⁰M. J. Joyce, M. Johnson, M. Gal, and B. F. Usher, *Phys. Rev. B* **38**, 10 978 (1988).
- ²¹V. A. Wilkinson, A. D. Prins, D. J. Dunstan, L. K. Howard, and M. T. Emeny, *J. Electron. Matter* **20**, 509 (1991).
- ²²G. Arnaud, J. Allègre, P. Lefebvre, H. Mathieu, L. K. Howard, and D. J. Dunstan, *Phys. Rev. B* **46**, 15 290 (1992).
- ²³W. S. Chi and Y. S. Huang, *Semicond. Sci. Technol.* **10**, 127 (1995), and references therein.
- ²⁴J. Leymarie, C. Monier, A. Vasson, A. M. Vasson, M. Leroux, B. Courboulès, N. Grandjean, C. Deparis, and J. Massies, *Phys. Rev. B* **51**, 13 274 (1995).
- ²⁵A. M. Vasson, A. Vasson, J. Leymarie, P. Disseix, P. Boring, and B. Gil, *Semicond. Sci. Technol.* **8**, 303 (1993).
- ²⁶D. Boffety, J. Leymarie, A. Vasson, A. M. Vasson, C. A. Bates, J. M. Chamberlain, J. L. Dunn, H. Henini, and O. H. Hughes, *Semicond. Sci. Technol* **8**, 1408 (1993).
- ²⁷W. H. Press, B. P. Flannery, S. A. Teukolsky, and W. T. Vetterling, *Numerical Recipes* (Cambridge University Press, Cambridge, England, 1987).
- ²⁸R. People and S. K. Spitz, *Phys. Rev. B* **41**, 8431 (1990).
- ²⁹K. H. Goetz, D. Bimberg, H. Jürgensen, J. Selders, A. V. Solomonov, G. F. Glinskii, and M. Razeghi, *J. Appl. Phys.* **54**, 4543 (1983).
- ³⁰C. Monier, P. Disseix, J. Leymarie, A. Vasson, A. M. Vasson, B. Courboulès, C. Deparis, M. Leroux, and J. Massies, *Proceedings of the International Conference on Semiconductor Heteroepitaxy, Montpellier, France, July 4–7, 1995* (Word Scientific, Singapore, 1995), p. 511.
- ³¹P. Bigenwald, P. Boring, K. J. Moore, B. Gil, and K. Woodbridge, *J. Phys. (France) IV* **4**, C2-215 (1994).
- ³²L. C. Andreani and A. Pasquarello, *Phys. Rev. B* **42**, 8928 (1990).
- ³³G. E. W. Bauer and T. Ando, *Phys. Rev. B* **38**, 6015 (1988).
- ³⁴L. Samuelson, M. Gerling, X. Liu, S. Nilsson, P. Omling, M. E. Pistol, and P. Silverberg, in *Proceedings of the 19th International Conference on the Physics of Semiconductors, Warsaw, Poland, August 15–19, 1988* (Institute of Physics Polish Academy of Science, Poland, 1988), p. 967.
- ³⁵C. G. Van de Walle, *Phys. Rev. B* **39**, 1871 (1989).
- ³⁶S. P. Kowalczyk, W. L. Shaffer, E. A. Kraut, and R. W. Grant, *J. Vac. Sci. Technol.* **20**, 705 (1982).
- ³⁷K. C. Hass, R. J. Lempert, and H. Ehrenreich, *Phys. Rev. Lett.* **52**, 77 (1984).